In-vivo conductivity of breast cancer and normal fibroglandular tissue using magnetic resonance electrical properties tomography: A comparison with apparent diffusion coefficient

So Yeon Won

Department of Medicine

The Graduate School, Yonsei University

In-vivo conductivity of breast cancer and normal fibroglandular tissue using magnetic resonance electrical properties tomography: A comparison with apparent diffusion coefficient

Directed by Professor Min Jung Kim

Doctoral Dissertation
submitted to the Department of Medicine,
the Graduate School of Yonsei University
in partial fulfillment of the requirements for the degree
of Doctor of Philosophy

So Yeon Won

June 2020

This certifies that the Doctoral Dissertation of So Yeon Won is approved.

Thesis Supervisor : Min Jung Kim

Thesis Committee Member#1 : Eun-Kyung Kim

Thesis Committee Member#2 : Joon Jeong

Thesis Committee Member#3: Dong-Hyun Kim

Thesis Committee Member#4: Ja Seung Koo

The Graduate School
Yonsei University

June 2020

ACKNOWLEDGEMENTS

I would like to express my gratitude towards my supervisor, professor Min Jung Kim, who has sincerely guided and encouraged me in completion of this paper.

I would like to thank professor Eun-Kyung Kim and Dong-Hyun Kim for sharing their knowledge and technical support.

I also want to express my gratitude to the committee members, professor Joon Jeong and Ja Seung Koo for sharing their precious time and comment during the period of my paper work.

<TABLE OF CONTENTS>

LIST OF FIGURES

LIST OF TABLES

ABSTRACT

In-vivo conductivity of breast cancer and normal fibroglandular tissue using magnetic resonance electrical properties tomography: A comparison with apparent diffusion coefficient

So Yeon Won

Department of Medicine
The Graduate School, Yonsei University

(Directed by Professor Min Jung Kim)

To evaluate the conductivity of normal breast parenchyma according to the menstrual cycle or menopausal status compared with ADC and to determine whether conductivity of normal breast tissue is affected by other clinicopathologic variables in patients with breast cancer.

This study included 102 breast cancer patients who had information about menstruation and underwent breast MRI for preoperative evaluation of breast cancer between July 2013 and December 2017. The normalized conductivity and ADCs of tumor and conductivity and ADCs of contralateral normal glandular tissue were measured and compared according to menopausal status (premenopausal and postmenopausal women) and menstruation cycles (1 to 4 weeks).

There were no significant differences in ADCs of contralateral normal glandular tissue between premenopausal and postmenopausal women ($p=0.534$) or among four menstrual weeks for premenopausal women ($p=0.534$). Conductivity of contralateral normal glandular tissue

showed a tendency to be higher in premenopausal women than in postmenopausal women but without significant difference (p=0.057).There were no significant difference in conductivity of normal fibroglandular tissue among four menstrual weeks for premenopausal women (p=0.800). Both of normalized conductivity and ADCs of breast cancer were not significantly different between premenopausal women and postmenopausal women (p=0.920, p=0.259, respectively) and between four menstruation weeks for premenopausal women (p=0.147, p=0.949, respectively). In multivariate analysis, mammographic density was an independent factor associated with ADC of contralateral normal breast (p=0.001). Mammographic density was an independent factor associated with conductivity of contralateral normal breast (p=0.001). Parenchymal enhancement, ER status and mammographic density were independent factor associated with normalized ADC of breast cancer (p=0.001, 0.013, 0.034).

There was no significant difference in the contralateral and normalized ADCs and contralateral and normalized conductivity during the menstruation cycles, suggesting that MRI can be performed at any time regardless of the menstruation cycle. Conductivity of normal breast parenchyma is a factor that is not affected by other various clinocopathologic factors, except breast density.

Key words : magnetic resonance electrical properties tomography, conductivity, apparent diffusion coefficient, normal fibroglandular tissue, breast cancer, menstruation cycle, menopausal state

In-vivo conductivity of breast cancer and normal fibroglandular tissue using magnetic resonance electrical properties tomography: A comparison with apparent diffusion coefficient

So Yeon Won

Department of Medicine
The Graduate School, Yonsei University

(Directed by Professor Min Jung Kim)

I. Introduction

Dynamic contrast-enhanced (DCE) breast magnetic resonance (MR) has been increasingly used to detect and diagnose breast cancer. The ACRIN 6666 study showed that additional mammography MRI screening increased cancer detection in women with a high risk of breast cancer[1]. The American Cancer Society recommended breast MRI screening for women with ≥20-25% lifetime risk of breast cancer or increased risk including BRCA mutation[2]. Contrast injection is usually required to detect breast cancer using breast MRI because it increases sensitivity and provides information about such conditions as perfusion [3]. However, gadolinium-based contrast agent may have various adverse effects, from mild to severe[4], including an increased risk for nephrogenic systemic fibrosis in patients with impaired renal function [5]. In addition, there has been a growing interest in gadolinium retention in tissues such as the brain, even without renal dysfunction [6,7]. Intravenous (IV) injection of contrast material makes patients uncomfortable. In healthy patients, these side effects are a barrier to the use of breast MRI for screening purposes.

Another obstacle is that background parenchymal enhancement (BPE) may affect diagnostic performance [8]. Although there are different conclusions on whether the menstruation cycles affect BPE [9,10], it is generally recommended to perform DCE breast MRI in week 2 of the menstrual cycle for the lowest background parenchymal enhancement [11-14]. This means the timing of breast MRI scans is important. Considering these shortcomings, the development of an imaging technique that can be used without contrast material for breast cancer screening is very meaningful. Diffusion weighted image (DWI) and magnetic resonance-based electrical properties tomography (MREPT) have been studied as alternative non-contrast imaging techniques.

DWI can be obtained by quantitatively measuring diffusivity of water molecules in tissues, known as apparent diffusion coefficient (ADC) without contrast agent. Breast cancers have lower ADCs than normal tissues [15-17]. A previous study showed unenhanced MRI with DWI have good sensitivity and specificity of breast cancer detection in asymptomatic patients and suggested that unenhanced MRI with DWI is a useful breast screening modality for patients who cannot use contrast material [18]. In DWI, several studies suggested that there was no significant difference in ADCs and tumor detectability between the proliferative and secretory phases of the menstrual cycle [19,20]. This means MRI can be performed at any time regardless of menstruation cycle, unlike dynamic breast MR in which BPE is influenced by menstruation cycle.

MREPT is another technique that has recently been investigated as an MR technique that does not use contrast material for screening. There have been studies on different dielectric properties of breast cancer and surrounding tissue, which showed that conductivity of malignant tissue was higher than that of normal tissue, suggesting the the diagnostic potential of this modality for breast cancer screening. [21,22]. Using MRI to measure conductivity was first described in 1991 [23]. In advance of a high-field MRI system, recently, MREPT has been actively investigated [24-26]. The basic concept of MREPT is that electric

properties of tissues distort B1 (component of RF field for spin excitation) and distorted B1 are measured using B1 mapping techniques [27]. MREPT has the advantage of obtaining conductivity using T2 weighted FSE phase axial image without any additional sequence, unlike ADC. Several studies on breast cancer have investigated the use of MREPT and shown its potential for clinical use [24,25,28,29]. However, little is known about the effect of clinicopathologic factors, including menstruation cycles or menopausal status, on conductivity values of both breast cancer and normal breast parenchyma for MREPT.

Because tissue conductivity is affected by cell membrane discharge, tissue necrosis, water contents, cell membrane breakdown and sodium concentration, it is likely that conductivity will be affected by change in tissue composition due to menstruation cycle or menopausal status [30]. Prior to the application of the MREPT as a screening modality, it is important to ensure it is not affected by hormonal cycle. So far, there have been studies on BPE and ADC of the normal breast tissue according to menstruation cycle or menopausal state, but no studies have been performed on whether conductivity is affected by the menstruation cycle or menopausal state. Our study is the first paper to evaluate conductivity, ADC, and BPE of the normal breast at the same time according to menstruation cycles. Therefore, the purpose of our study was to evaluate the conductivity of normal breast parenchyma according to the menstrual cycle or menopausal status compared with ADC and to determine whether conductivity of normal breast tissue is affected by other clinicopathologic variables in patients with breast cancer.

II. Material and methods

1. Patients

This retrospective study was approved by the Severance Hospital Institutional Review Board. The requirement for informed consent was waived.

Between July 2013 and December 2017, patients who underwent breast MRI for preoperative evaluation of pathologically diagnosed breast cancer prior to diagnostic core biopsy or therapeutic surgery were reviewed (n=447). We excluded patients lacking definitive information about menstruation, including last menstrual period, or those with irregular menstruation cycles (n=185). The remaining 262 patients were divided into a premenopausal group (n=118) and a postmenopausal group (n=144). In the premenopausal group, following patients were excluded: 1) those with invasive breast carcinomas <2 cm on T2-weighted FSE (n=45) (tumors <2 cm were excluded considering boundary effect on conductivity, low spatial resolution, chemical shift artifact and lack of signal to nose ratio) [25,31] and 2) those with missing data or data errors (n=17). In the postmenopausal group, following patients were excluded: 1) those experiencing menopause within ≤2 years from the date of the study (n= 56), 2) those with breast cancer <2 cm when measuring size of breast cancer on T2-weighted FSE (n=36), and 3) those with missing data or data errors (n=6). A total of 56 premenopausal and 46 postmenopausal women were included. Premenopausal group was divided into four groups according to menstruation cycles.

2. Image acquisition

Breast MRI examinations were performed on a 3.0-T system (MR750, GE Healthcare, Waukesha, WI, USA) using an 8 channel breast receiver coil. The baseline breast MRI sequentially consisted of T2-weighted fast spin echo axial images (used to acquire raw data for this study, TR/TE, 9,100/ 100 msec; flip angle, 110°; field of view (FOV), 320 mm; matrix, 416×256 pixels; slice thickness, 3 mm; with no slice gap; acquisition time, 3 min 30 s), T2-stimulated inversion recovery axial images (TR/TE, 5,000/70 msec; inversion time, 200 msec; flip angle, 110°; FOV, 320 mm; matrix, 320×256 pixels; slice thickness, 3 mm; with no slice gap; acquisition time, 3 min 12 s), DW images using a

single shot echo planar imaging (b=0 and 600 s/mm2; TR/TE, 6, 000/70 msec; FOV, 320 mm; matrix, 128×128; slice thickness, 3 mm; with no slice gap; acquisition time, 3 min 40 s), and T1-weighted non-fat-suppressed pre-contrast and 3D dynamic post-contrast-enhanced (DCE) axial images [flip angle, 12°; FOV, 320 mm; matrix, 280×512 pixels; slice thickness, 3 mm; with no slice gap; acquisition time, 8 min 17 s; obtained before and after a bolus injection of 0.2 mmol/kg body weight of gadolinium-based contrast agent (Dotarem, Guerbet, Paris, France; Magnevist, Berlex Laboratories, Wayne, NJ, USA; or Gadovist, Bayer Schering Pharma, AG, Berlin, Germany) at a rate of 1 or 2 ml/sec according to concentration, followed by a 20-ml saline flush].

3. Conductivity reconstruction using phase-based electric properties tomography (EPT)

Our study used phase-based EPT [26], which is a technique to reconstruct an *in-vivo* conductivity map using only transceive phase mapping. Before the reconstruction, however, the coil-combination technique is required for reducing the errors caused by the use of a multichannel receiver [25,32]. In this study, a subject-specific coil-combination[32] is applied and then phase-based EPT is performed with adaptive fitting [24,25]. Previous studies [25,32] validated the feasibility of the overall process for phase-based EPT.

4. Image analysis

The conductivity and ADC were measured in malignant breast lesions and normal fibroglandular tissue in the contralateral breast. To measure conductivity, postprocessing and setting of region of interest (ROI) were conducted using MatLab (MathWorks, Natick, MA). ROI was manually drawn in the T2 weighted FSE phase axial image and the ADC map, because conductivity was reconstructed using T2 weighted FSE phase data (Figure 1,2).

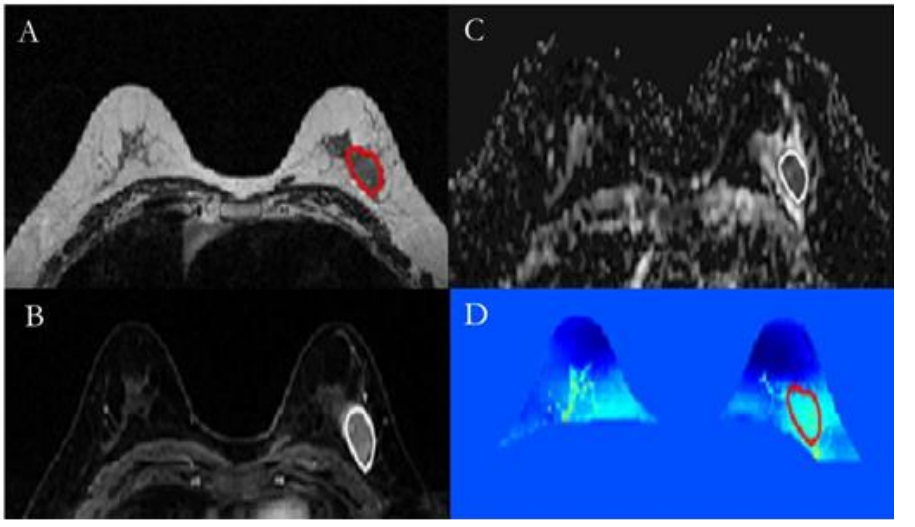

Figure 1. ROI in breast cancer. (A) T2-weighted fast spine echo image demonstrating iso- to hypo-intense mass with respect to breast parenchyma. (B) 3D dynamic post-contrast-enhanced (DCE) axial images (C) ADC map demonstrating mass with low signal intensity. (D) Conductivity map showing a mean conductivity value.

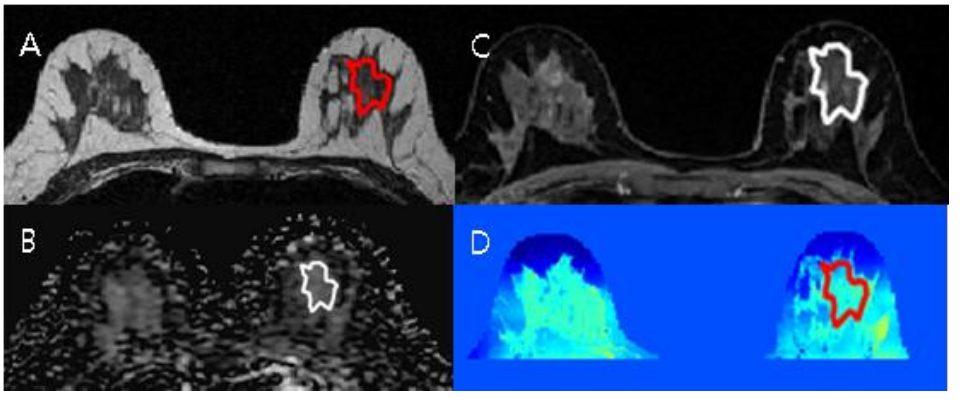

Figure 2. ROI in normal fibroglandular tissue. (A) T2-weighted fast spine echo image demonstrating iso- to hypo-intense mass with respect to breast parenchyma. (B) 3D dynamic post-contrast-enhanced (DCE) axial images (C) ADC map demonstrating mass with low signal intensity. (D) Conductivity map showing a mean conductivity value.

Cross-section with the largest diameter tumor was chosen. To measure conductivity, polygonal shaped ROIs were drawn within cancer lesions to include most, though not all, of the tumor to avoid partial volume effect. We drew the ROI on the T2 weighted FSE phase axial image and ADC map with reference to the first or second phase of contrast-enhanced sequence. In case of a tumor with cystic or necrotic component, the ROI was drawn with discretion to avoid the cystic component by comparing it to the T2 weighted image, as much as possible. To measure conductivity and ADCs of normal fibroglandular tissue in contralateral breast, ROIs were also manually drawn in the T2 weighted FSE phase axial image and ADC map. The cross-section including as much breast parenchyma as possible was chosen. The ROIs were drawn in homogenous breast parenchyma at chosen cross-sectional images. Referring to the T1 weighted image, ROIs were carefully drawn to avoid fatty tissue as much as possible. Under the supervision of one radiologist (M.J.K with 16_years of experience), one senior resident radiologist (S.Y.W) in breast MRI manually drew all ROIs on the selected slice of the T2-weighted FSE and ADC map.

5. Data analysis

Clinicopathologic data, including mean age, body mass index (BMI), tumor size, menopausal status, menstruation cycle, BPE, mammographic density, tumor marker (estrogen receptor (ER), progesterone receptor (PR), HER-2 and Ki-67), pathologic type, nuclear and histologic grades, and lymphovascular invasion (LVI), were collected from medical records.

Patients were classified into the premenopausal or postmenopausal groups. In premenopausal women, patients were divided into four groups according to their week of menstruation (from 1^{st} week to 4^{th} week). Mammographic density was divided into fatty breast (Bi_RADS A&B) and dense breast (Bi_RADS C&D) according to the amount of fibroglandular tissue

[33]. Histological and nuclear grades were divided into two groups: low (grade 1–2) and high (grade 3). When tumors had >9 % ER-positive cells in immunohistochemical stains (IHC), the cancer was defined as ER-positive[34]. PR-positive cancers were similarly defined when tumors had >9% PR-positive cells in IHC. When the result was 3+ in IHC for HER-2, the cancer was defined as HER-2-positive. When the result was 0 or 1 in IHC for HER-2, the cancer was defined as HER-2-negative. If the result was 2+, we referred to florescent in situ hybridization (FISH). When FISH had a value of >2.0, the cancer was defined as HER-2-positive. Ki-67-positivity was defined as Ki-67 levels of >14%. Nuclear and histologic grades were divided into not high (grade 1 and grade 2) and high (grade 3). We selected and modified the concept of normalized ADC as it was suggested to improve the characterization of breast lesions[35]. The concept was also applied to conductivity. Normalized ADC (ADCn)= ADC of breast cancer (ADCc)/ADC of contralateral normal glandular tissue (ADCg). Normalized conductivity= Conductivity of breast cancer/Conductivity of contralateral normal glandular tissue.

All clinicopathologic factors were compared according to menopausal status and menstruation cycles. Shapiro-Wilk test for normality and Levene's F test for equal variance were performed for continuous data. Mann-Whitney U test or Kruskal-Wallis test were used for data without normality and equal variance such as BMI and radiologic tumor size. Student's t test or analysis of variance was used for continuous data with normality and equal variance such as mean age. For categorical variables such as BPE, mammographic density, tumor marker, pathologic type, lymphovascular invasion (LVI), and nuclear and histologic grades, chi-square test or Fisher's exact text was used. Spearman's correlation, Mann-Whitney U test, and Kruskal-Wallis test were used to evaluate the relationship between ADC or conductivity and other clinicopathologic factors. After confirming normality and equal variance, Student's t test was used. Pearson correlation was performed to determine

whether age was correlated to contralateral and normalized ADCs and contralateral and normalized conductivity. Spearman correlation was performed to determine whether BMI and radiologic tumor size were correlated to contralateral and normalized ADCs and contralateral and normalized conductivity. Student's t test was performed to determine whether mammographic density was correlated with ADC of contralateral normal breast or conductivity of contralateral normal breast. Mann-Whitney U test was performed to evaluate whether other clinicopathologic factors were correlated to contralateral and normalized ADCs and contralateral and normalized conductivities.

Multivariate analysis was performed using significant factors in univariate analysis to evaluate independent factors associated with conductivity and ADCs. If the *p*-value was <0.05, it was considered statistically significant. All statistical analyses were performed with SPSS version 25.0.

III. Results

1. Comparison of clinicopathologic features between the premenopausal and postmenopausal groups

Table 1 lists clinicopathologic features of the 102 patients. Of these women, 56 (54.9%) were premenopausal and 46 (45.1%) were postmenopausal (Table 1). The proportion of patients with ER- and PR-positive cancers was higher in the premenopausal group than in the postmenopausal group (p=0.041, 0.003 Table 1). The proportion of dense breast and strong BPE were also higher in the premenopausal group than in the postmenopausal group (p=0.001, p<0.001, respectively, Table 1).

Table 1. Clinicopathologic features of the 102 patients

Characteristics		Total	Premenopause (n=56)	Menopause (n=46)	p-value
Age (years)		50.64 ± 11.71	41.38±6.94	60.80±7.69	**<0.001**
BMI (Kg/m2)		22.05 (20.70-24.05)	21.83 (20.69-23.58)	22.70 (20.66-24.52)	0.538
Radiologic tumor size(cm)		2.9 (IQR 2.0-4.0)	2.9 (2.2-4.5)	3.0(2.5-4.1)	0.976
Parenchymal enhancement of MRI	1	61 (59.8)	16 (28.6)	45 (97.8)	**<0.001**
	2	23 (22.5)	22 (39.3)	1 (2.2)	
	3	15 (14.7)	15 (26.8)	0 (0.0)	
	4	3 (2.9)	3 (5.4)	0 (0.0)	
Tumor location	Rt	45 (44.1)	28 (50.0)	29 (63.0)	0.187
	Lt	57 (55.9)	28 (50.0)	17 (37.0)	
Mammographic density	Fatty breast	12 (11.8)	1 (1.8)	11 (23.9)	**0.001**
	Dense breast	90 (88.2)	55 (98.2)	35 (76.1)	
ER	Negative	42 (41.2)	18(32.1)	24(52.2)	0.041
	Positive	60 (58.8)	38(67.9)	22(47.8)	
	N/A	0 (0.0)	0 (0.0)	0 (0.0)	
PR	Negative	66 (64.7)	29(51.8)	37(80.4)	0.003
	Positive	36 (35.3)	27(48.2)	9(19.6)	
	N/A	0 (0.0)	0 (0.0)	0 (0.0)	
HER-2	Negative	64 (62.7)	39 (69.6)	25 (54.3)	0.081
	Positive	31 (30.4)	13 (23.2)	18 (39.1)	
	N/A	7 (6.9)	4 (7.1)	3 (6.5)	
Ki-67	Negative	36 (35.3)	20 (35.7)	16 (34.8)	0.761
	Positive	46 (45.1)	24 (42.9)	22 (47.8)	
	N/A	20 (19.6)	12 (21.4)	8 (15.2)	
Pathology	IDC	92 (90.2)	49 (87.5)	43 (93.5)	0.739
	ILC	2 (2.0)	1 (1.8)	1 (2.2)	
	DCIS	8 (7.8)	6 (10.7)	2 (4.3)	
Nuclear	Not high	47 (46.1)	26 (46.4)	21 (45.7)	0.949

grade	High	48 (47.1)	26 (46.4)	22 (47.8)	
	N/A	7 (6.9)	4 (7.1)	3 (6.5)	
Histologic grade	Not high	58 (56.9)	31(55.4)	27(58.7)	0.879
	High	29 (28.4)	15 (26.8)	14 (30.4)	
	N/A	15 (14.7)	10 (17.9)	5 (10.9)	
Lymphovascular invasion	Absent	89 (87.3)	49 (87.5)	40 (87.0)	1.000
	Present	8 (7.8)	4 (7.1)	4 (8.7)	
	N/A	5 (4.9)	3 (5.4)	2 (4.3)	

2. Comparison of clinicopathologic features according to menstrual cycles in premenopausal women

There was no significant difference in clinicopathologic features according to menstruation cycles in premenopausal women (Table 2). In subgroup analysis (BPE degree 1 vs. 2,3,4), comparing the second week group with the lowest tendency of BPE and the fourth week group with the highest tendency of BPE, the fourth week group (40%) had a lower percentage of BPE 1 than the second week group (0.0%; p=0.058).

Table 2. Clinicopathologic features of 56 premenopausal women according to menstruation cycles

		Premenopausal (n=56)					
		Week 1 (n=20)	Week 2 (n=15)	Week 3 (n=13)	Week 4 (n=8)	P value	Total (n=56)
Age		42.40 ±6.64	43.00 ±6.48	40.46 ±5.94	37.25 ±9.19	0.232	41.38±6.9
BMI		22.73 (20.70-24.13)	21.83 (21.19-22.72)	21.11 (20.20-23.09)	23.42 (19.12-26.55)	0.610	21.83 (20.69-23.58)
Parenchymal enhancement of MRI	1	6 (30.0)	6 (40.0)	4 (30.8)	0 (0.0)	0.607	16 (28.6)
	2	9 (45.0)	4 (26.7)	5 (38.5)	4 (50.0)		22 (39.3)
	3	4 (20.0)	4 (26.7)	4 (30.8)	3 (37.5)		15 (26.8)
	4	1 (5.0)	1 (6.7)	0 (0.0)	1 (12.5)		3 (5.4)

Mammographic density	Fatty	0 (0.0)	0 (0.0)	1 (7.7)	0 (0.0)	0.375	1 (1.8)
	Dense	20 (100.0)	15 (100.0)	12 (92.3)	8 (100.0)		55 (98.2)
ER	Negative	4 (20.0)	5 (33.3)	4 (30.8)	5 (62.5)	0.221	18 (32.1)
	Positive	16 (80.0)	10 (66.7)	9 (69.2)	3 (37.5)		38 (67.9)
PR	Negative	9 (45.0)	7 (46.7)	6 (46.2)	7 (87.5)	0.193	29 (51.8)
	Positive	11 (55.0)	8 (53.3)	7 (53.8)	1 (12.5)		27 (48.2)
HER-2	Negative	13 (65.0)	11 (73.3)	8 (61.5)	7 (87.5)	0.599	39 (69.6)
	Positive	6 (30.0)	2 (13.3)	4 (30.8)	1 (12.5)		13 (23.2)
	N/A	1(5.0)	2 (13.3)	1 (7.7)	0		4(7.1)
Ki-67	Negative	8 (50.0)	6 (40.0)	5 (38.5)	1 (12.5)	0.451	20 (35.7)
	Positive	7 (35.0)	5 (33.3)	7 (53.8)	5 (62.5)		24 (42.9)
	N/A	5(25.0)	4(26.7)	1(7.7)	2(25.0)		12(21.4)
Pathology	IDC	18 (90.0)	12 (80.0)	11 (84.6)	8 (100.0)	0.758	49 (87.5)
	ILC	0 (0.0)	0 (0.0)	1 (0.0)	0 (0.0)		1 (1.8)
	DCIS	2 (10.0)	3 (20.0)	1 (7.7)	0 (0.0)		6 (10.7)
Nuclear grade	Not high	10 (50.0)	4 (26.7)	10 (76.9)	2 (25.0)	0.073	26 (46.4)
	High	9 (45.0)	8 (53.3)	3 (23.1)	6 (75.0)		26 (46.4)
	N/A	1 (5.0)	3 (2.0)	0 (0.0)	0 (0.0)		4(7.2)
Histologic grade	Not high	13 (65.0)	6 (40.0)	8 (61.5)	4 (50.0)	0.650	31 (55.4)
	High	4 (20.0)	3 (20.0)	4 (30.8)	4 (50.0)		15 (26.8)
	N/A	3 (15.0)	6(40.0)	1 (7.7)	0 (0.0)		10 (17.9)
Lymphovascular invasion	Absent	18 (90.0)	12 (80.0)	11 (84.6)	8 (100.0)	0.568	49 (87.5)
	Present	2 (10.0)	0 ()	2 (15.4)	0 (0.0)		4 (7.1)
	N/A	0	3 (20.0)	0	0		3 (5.4)

3. Comparison of ADCs between breast cancer and contralateral normal fibroglandular tissue

Average ADCs were significantly lower in breast cancer tissue (median: 1039.9, IQR: 928.6-1177.9) than in normal parenchyma (median: 1644.3, IQR: 1419.3-1815.5, $p<0.001$) (Figure 3).

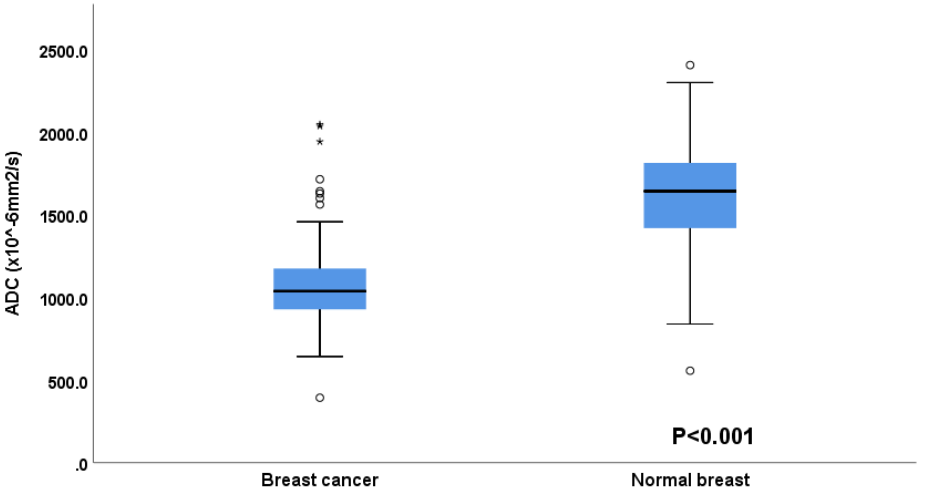

Figure 3. Comparison of ADCs between breast cancer and normal glandular tissues

4. Comparison of ADCs of the normal fibroglandular tissue according to menopausal status or menstruation cycles

There were no significant differences in ADCs of contralateral normal glandular tissue between premenopausal and postmenopausal women (median 1651.7, 1637.5, p=0.534, Figure 4), or among 4 menstrual weeks for premenopausal women (median 1619.2, 1644.2, 1737.2, 1560.5, p=0.534, Table 3, Figure 5). In subgroup analysis comparing the week 2 and week 4 groups, ADC of contralateral normal breast was not significantly different in the two groups (p=0.591).

Table 3. ADCs according to menopausal status and menstrual cycle

	Premenopausal						Postmenopausal (n=46)	P value
Median ADC values (IQR)	Week1 (n=20)	Week2 (n=15)	Week3 (n=13)	Week4 (n=8)	P value*	Subtotal (n=56)		
ADC of contralateral normal breast	1619.2 (1476.2-1885.7)	1644.2 (1390.0-1851.3)	1737.2 (1364.2-1900.8)	1560.5 (1301.0-1720.3)	0.534	1651.7 (1423.6-1842.5)	1637.5 (1389.7-1774.5)	0.534
Normalized ADC of breast cancer	0.654 (0.575-0.774)	0.628 (0.571-0.751)	0.613 (0.573-0.729)	0.604 (0.521-0.838)	0.949	0.622 (0.572-0.761)	0.707 (0.528-0.838)	0.259

P-value*: comparison among menstruation cycles.

P-value: comparison between premenopausal and postmenopausal women.

Normalized ADC = ADC of breast cancer tissue/ADC of contralateral normal breast

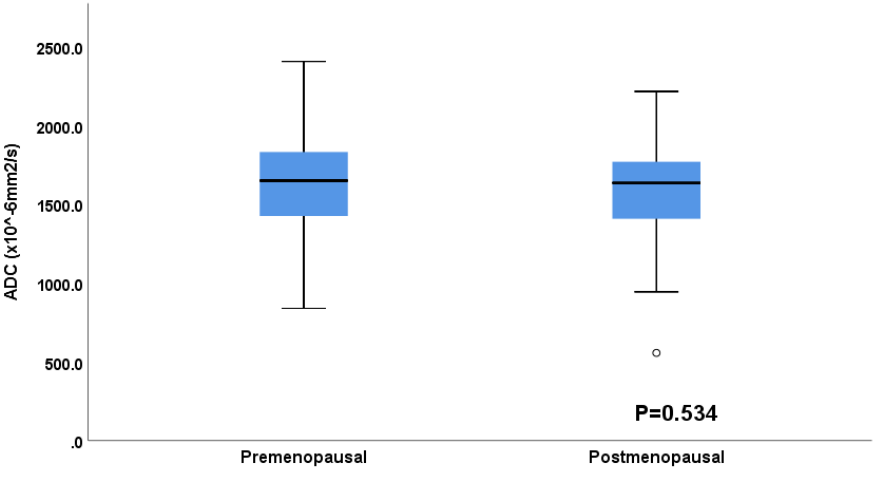

Figure 4. Comparison of ADCs of normal breast according to menopausal status.

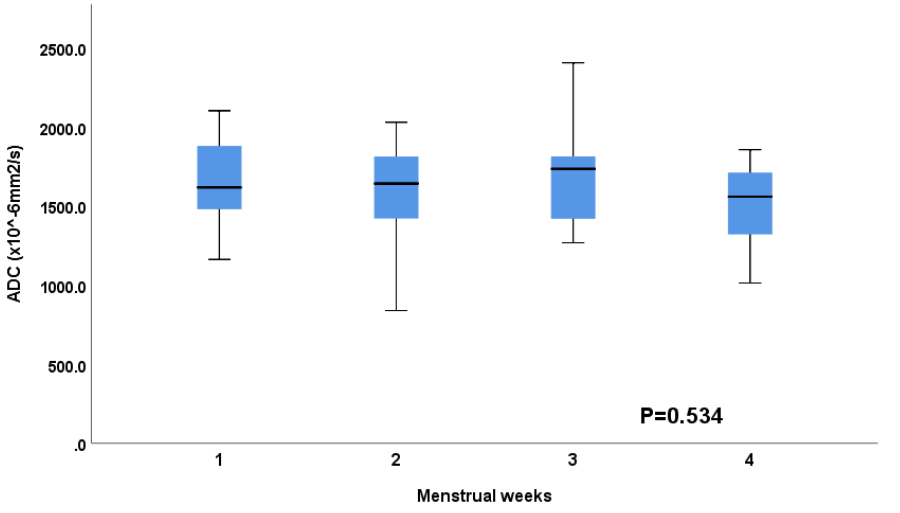

Figure 5. Comparison of ADCs of normal breast according to menstruation cycles.

5. Comparison of normalized ADCs of breast cancer according to menopausal status or menstruation cycles

There was no significant difference for normalized ADCs between premenopausal and postmenopausal women (median 0.622, 0.707, p=0.259, Figure 6), or among the 4 menstrual weeks for premenopausal women (median 0.654, 0.628, 0.613, 0.604, p=0.949, Table 3, Figure 7).

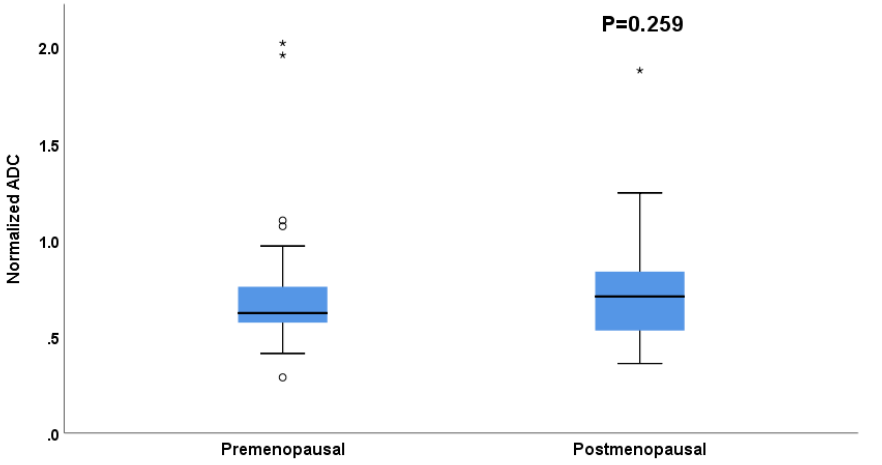

Figure 6. Comparison of normalized ADCs of breast cancer according to menopausal status.

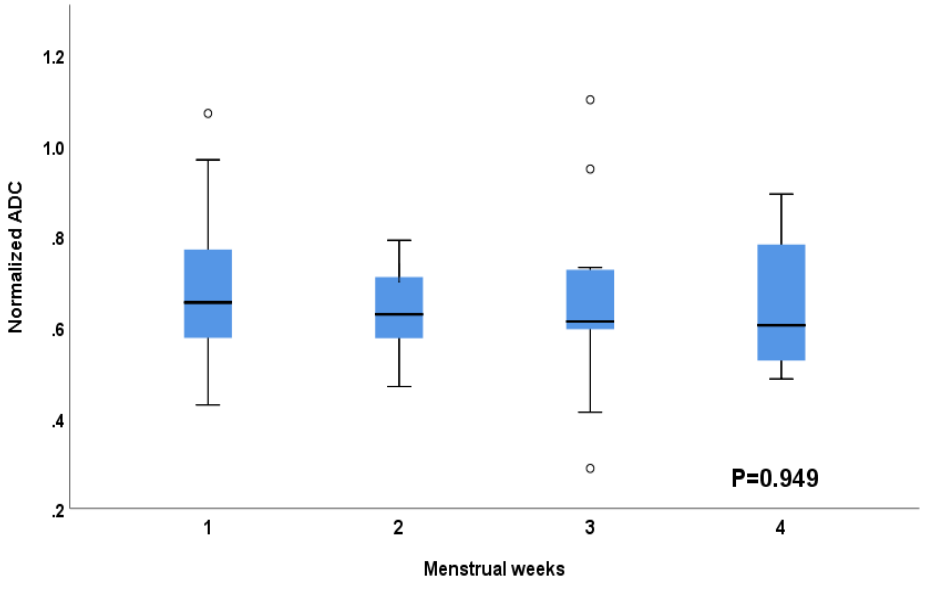

Figure 7. Comparison of normalized ADCs of breast cancer according to menstruation cycles.

6. Univariate and multivariate analysis of factor affecting ADC of normal breast

In univariate analysis, BMI and breast density were associated with ADC of normal breast (Table 4). Patients with lower BMI and dense breast had higher ADC than those with higher BMI and fatty breast (p=0.027, <0.001).

Table 4. Univariate analysis of variables independently associated with ADC of normal fibroglandular tissues

		Patient number (n=102)	Correlation coefficient with ADC values (rho,ρ)	Median ADC values	P value
Age			-0.041		0.680
BMI			-0.219		**0.027**
Parenchymal enhancement	1	61		1650.60 (1439.9-1817.6)	0.277
	2	23		1636.10 (1420.80-1851.30)	
	3	15		1627.70 (1363.80-1800.30)	
	4	3		1163.80 (1014.60-)	
Menopausal state	Premenopausal	56		1651.65 (1423.60-1842.45	0.534
	Postmenopausal	46		1637.45 (1389.68-1774.45)	
Menstruation cycle	1 week	20		1619.20 (1476.15-1885.73)	0.534
	2 week	15		1644.20 (1390.00-1851.30)	
	3 week	13		1737.20 (1364.2-1900.8)	
	4 week	8		1560.50 (1301.0-1720.30)	
Mammographic density	Fatty breast	12		1294.02±353.24	**<0.001**
	Dense breast	90		1649.89±298.48	

In multivariate analysis, mammographic density was an independent factor associated with ADC of normal breasts (p=0.001, Table 5), and a high BMI was associated with lower ADC, with borderline significance (p=0.072).

Table 5. Multivariate analysis of variables independently associated with ADC of normal fibroglandular tissues

	Beta coefficient	Standard error	P value
Postmenopausal	24.659	64.140	0.701
BMI(Kg/m2)	-18.355	10.093	0.072
Dense breast on mammogram	343.198	99.918	**0.001**

7. Univariate and multivariate analysis of factor affecting normalized ADC of breast cancers

In univariate analysis, radiologic tumor size, ER, PR, and mammographic density were associated with normalized ADC (Table 6). Patients with large tumor size, ER-negative cancer, PR-negative cancer, and fatty breast had higher ADC than those with small tumor size, ER-positive cancer, PR-positive cancer, and dense breast (p=0.008, 0.002, 0.039, 0.028, table 6).

Table 6. Univariate analysis of variables independently associated with normalized ADC of breast cancer

	Patient number (n=102)	Correlation coefficient with ADC values (rho,ρ)	Median ADC values	P value
Age		-0.062		0.534
BMI		-0.050		0.616

Radiologic tumor size(cm)			0.266	**0.008**
Parenchymal enhancement of MRI	1	61	0.668 (0.525-0.781)	0.089
	2	23	0.664 (0.538-0.777)	
	3	15	0.671 (0.596-0.792)	
	4	3	0.686 (0.603-)	
Menopausal state	Premenopausal	56	0.622 (0.572-0.761)	0.259
	Postmenopausal	46	0.707 (0.528-0.838)	
Menstruation cycle	1 week	20	0.654 (0.575-0.774)	0.949
	2 week	15	0.628 (0.571-0.751)	
	3 week	13	0.613 (0.573-0.729)	
	4 week	8	0.604 (0.521-0.838)	
Mammographic density	Fatty breast	12	0.761 (0.679-0.932)	**0.028**
	Dense breast	90	0.642 (0.537-0.772)	
ER	Negative	42	0.719 (0.629-0.862)	**0.002**
	Positive	60	0.609 (0.514-0.740)	
PR	Negative	66	0.673 (0.555-0.831)	**0.039**
	Positive	36	0.600 (0.556-0.747)	
HER-2	Negative	64	0.614 (0.537-0.781)	0.162
	Positive	31	0.704 (0.616-0.780)	
	N/A	7		

Ki-67	Negative	36	0.655 (0.533-0.789)	0.830
	Positive	46	0.662 (0.558-0.794)	
	N/A	20		
Pathology	IDC	92	0.661 (0.563-0.782)	0.304
	ILD	2	0.486 (0.367-)	
	DCIS	8	0.673 (0.558-0.809	
Nuclear grade	Not high	47	0.671 (0.551-0.797)	0.693
	High	48	0.657 (0.521-0.789)	
	N/A	7		
Histologic grade	Not high	58	0.662 (0.547-0.802)	0.679
	High	29	0.650 (0.526-0.761)	
	N/A	15		
Lymphovascular invasion	Absent	89	0.656 (0.544-0.787)	0.954
	Present	8	0.698 (0.518-0.878)	
	N/A	5		

In multivariate analysis, parenchymal enhancement, ER group, and mammographic density were independent factor associated with normalized ADC (0.119, p=0.001; -0.149, p=0.013; -0.167, p=0.034, Table 7).

Table 7. Multivariate analysis of variables independently associated with normalized ADC of breast cancer

	Beta coefficient	Standard error	P value
Radiologic tumor size(cm)	0.015	0.012	0.209
Parenchymal enhancement	0.119	0.036	**0.001**

ER(+)	-0.149	0.059	**0.013**
PR (+)	0.001	0.063	0.985
Postmenopausal	0.118	0.063	0.066
Dense breast on mammogram	-0.167	0.078	**0.034**

8. Comparison of conductivity between breast cancer and contralateral normal fibroglandular tissue

Average conductivity values were significantly higher in breast cancer tissue (0.389±0.195) than in normal contralateral glandular tissue (0.243±0.226, $p<0.001$, Figure 8).

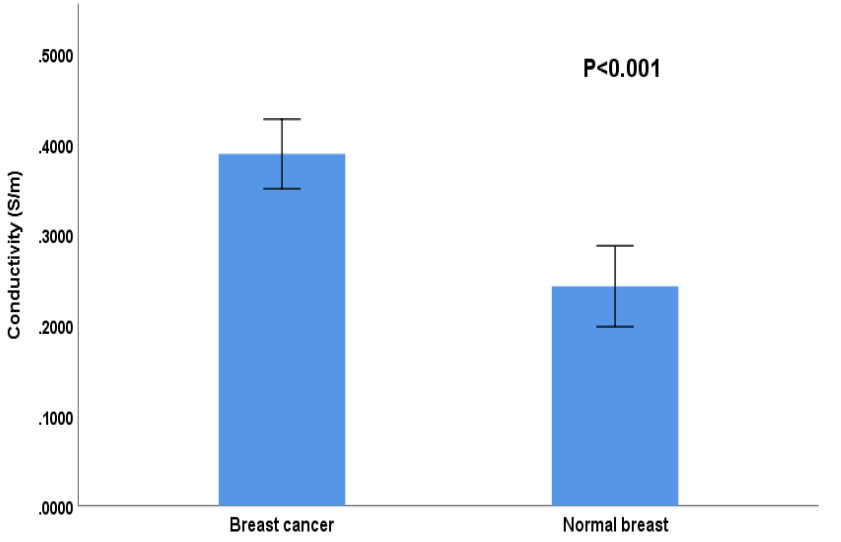

Figure 8. Comparison of conductivity between breast cancer and normal glandular tissue.

9. Comparison of conductivity of normal fibroglandular tissue according to menopausal status or menstruation cycles

Conductivity of contralateral normal glandular tissue showed a tendency to be higher in premenopausal women than in postmenopausal women (0.248, 0.187, Figure 9) but without significant difference (p=0.057). In premenopausal women, there was no significant difference among the four menstrual weeks (0.223, 0.293, 0.201, 0.254, p=0.800, Table 8, Figure 10). In subgroup analysis comparing the week 2 and week 4 groups, conductivity of contralateral normal breast was not significantly different in the two groups (p=0.428).

Table 8. Conductivity values according to menopausal status and menstrual cycle

	Premenopausal						postmenopausal	P value
	Week1 (n=20)	Week2 (n=15)	Week3 (n=13)	Week4 (n=8)	P value*	Subtotal (n=56)	(n=45)	
Conductivity of contralateral normal breast	0.223 (0.163-0.509)	0.293 (0.120-0.537)	0.201 (0.063-0.414)	0.254 (0.111-0.452)	0.800	0.248 (0.152-0.458)	0.187 (0.087-0.337)	0.057
Normalized conductivity of breast cancer	1.642 (1.033-2.575)	1.170 (0.804-3.363)	1.036 (0.436-1.877)	0.997 (0.786-1.433)	0.147	1.213 (0.820-2.458)	1.255 (0.710-2.407)	0.920

*In one postmenopausal patient, conductivity data of contralateral normal breast were lost due to processing error.

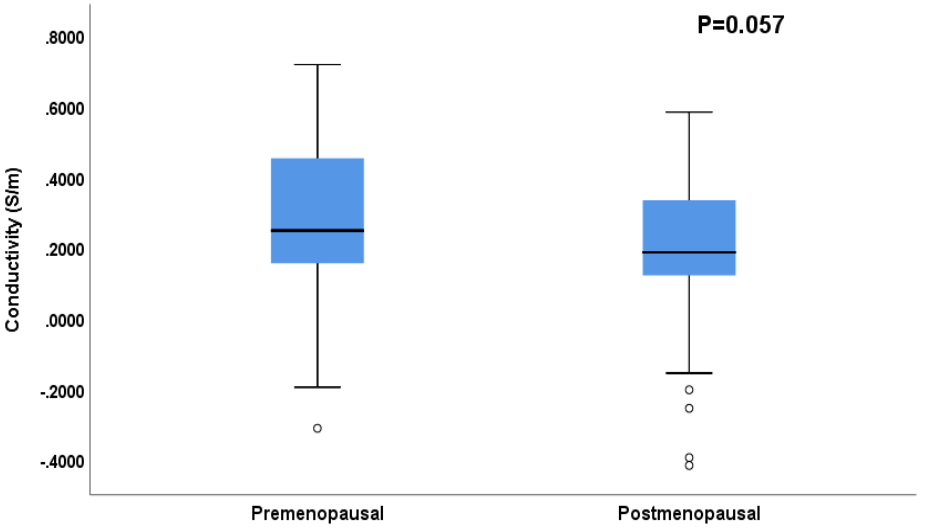

Figure 9. Comparison of conductivity of normal breast according to menopausal status.

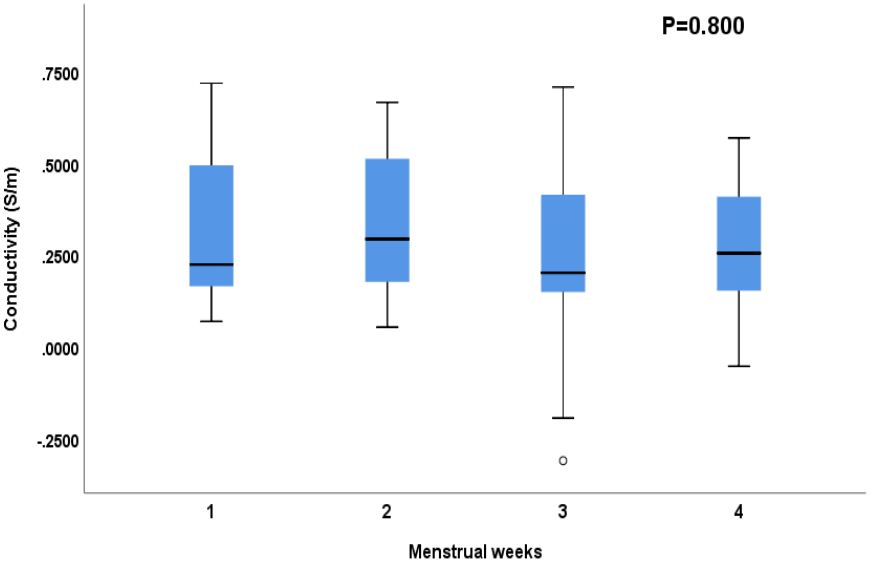

Figure 10. Comparison of conductivity of normal breast according to menstruation cycles.

10. Comparison of normalized conductivity of breast cancer according to menopausal status or menstruation cycles

Normalized conductivity of breast cancer was not significantly different between premenopausal and postmenopausal women (1.213, 1.255, p=0.920, Table 3, Figure 11) and between the four menstruation weeks for premenopausal women (1.642, 1.170, 1.036, 0.997, p=0.147, Table 3, Figure 12).

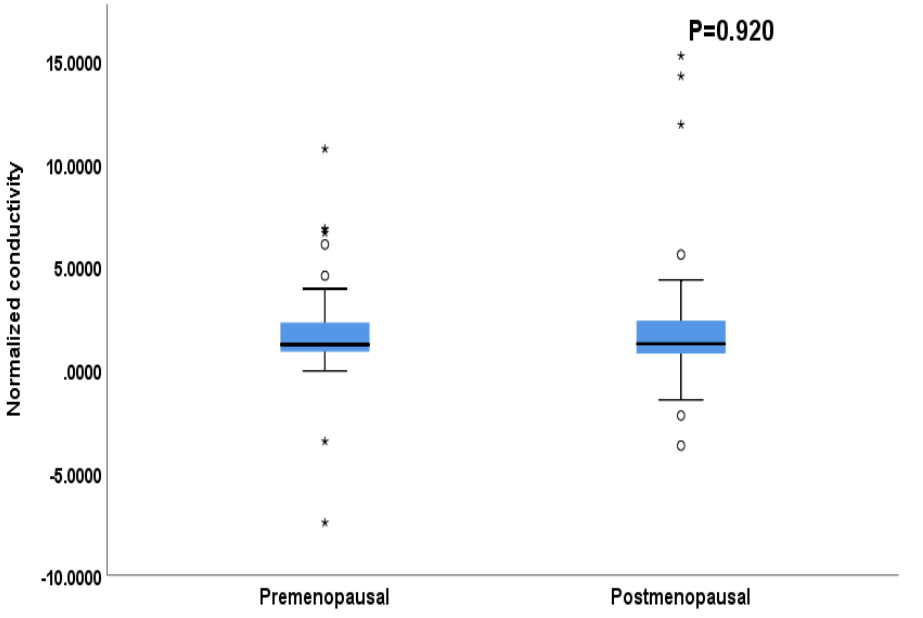

Figure 11. Comparison of normalized conductivity of breast cancers according to menopausal status.

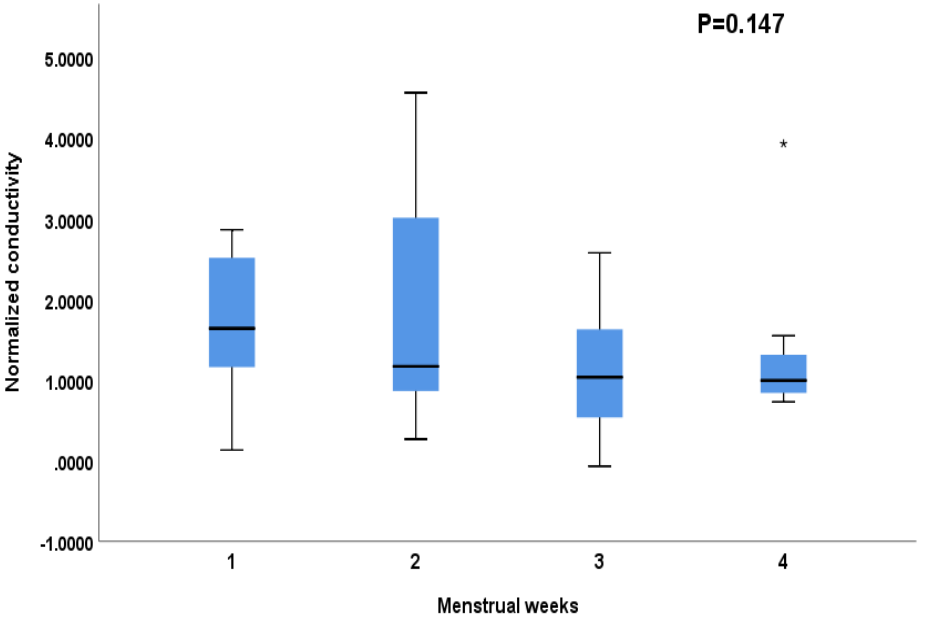

Figure 12. Comparison of normalized conductivity of breast cancers according to menstruation cycles.

11. Univariate and multivariate analysis of factor affecting conductivity of normal breast

In univariate analysis, age, BMI, and mammographic density were associated with conductivity of normal fibroglandular tissue (Table 9). Patients with younger age and lower BMI had higher conductivity than those with older age and higher BMI (ρ=-0.026, -0.352; p=0.010, <0.001), and those with dense breast had higher conductivity than those with fatty breast. (mean conductivity: -0.015 (fatty breast), 0.274 (dense breast), p<0.001).

Table 9. Univariate analysis of variables independently associated with conductivity of normal fibroglandular tissues

		Patient number (n=101*)	Correlation coefficient with conductivity values (rho,ρ)	Beta coefficient	Standard error	Mean	P value
Age			-0.026				**0.010**
BMI			-0.352				**<0.001**
Parenchymal enhancement	1	60				0.220 (0.129-0.342)	0.416
	2	23				0.253 (0.168-0.415)	
	3	15				0.255 (0.103-0.537)	
	4	3				0.120 (0.068-)	
Menopausal state	premenopausal	56				0.248 (0.152-0.458)	0.057
	Postmenopausal	45				0.187 (0.087-0.337)	
Menstruation cycle	1 week	20				0.223 (0.163-0.509)	0.681
	2 week	15				0.293 (0.120-0.537)	
	3 week	13				0.201 (0.063-0.414)	
	4 week	8				0.254 (0.111-0.452	

					)	
Mammographic density	Fatty breast	11			-0.015±0.275	**<0.001**
	Dense breast	90	0.289	0.067	0.274±0.120	

*In one postmenopausal patient, conductivity data of contralateral normal breast were lost due to processing error.

In multivariate analysis, mammographic density was an independent factor associated with conductivity of normal breasts (p=0.001, Table 10), and a high BMI was associated with lower conductivity, with borderline significance (p=0.082).

.

Table 10. Multivariate analysis of variables associated with conductivity of normal fibroglandular tissues

	Beta coefficient	Standard error	P value
Postmenopausal	0.003	0.071	0.965
Age(year)	-0.003	0.003	0.329
BMI(Kg/m2)	-0.012	0.007	0.082
Dense breast on mammogram	0.224	0.007	**0.001**

12. Univariate analysis of factor affecting normalized conductivity of breast cancer

No factor was associated with normalized conductivity in univariate analysis. Multivariate analysis was not performed due to the absence of a significant factor in univariate analysis (Table 11).

Table 11. Univariate analysis of variables independently associated with normalized conductivity of 100 breast cancer

		Patient number (n=100*)	Correlation coefficient with normalized conductivity values (rho,ρ)	Mean	P value
Age			0.155		0.123
BMI			0.143		0.152
Radiologic tumor Size			-0.058		0.571
Parenchymal enhancement	1	60		1.262 (0.979-2.419)	0.201
	2	23		0.951 (0.684-1.642)	
	3	14		1.420 (0.711-2.982)	
	4	3		3.363 (1.026-)	
Menopausal status	Premenopausal	55		1.213 (0.820-2.458)	0.920
	Postmenopausal	45		1.255 (0.710-2.407)	
Menstruation cycle	week 1	19		1.642 (1.033-2.575)	0.133
	Week 2	15		1.170 (0.804-3.363)	
	Week 3	13		1.036 (0.436-1.877)	
	Week 4	8		0.997 (0.786-1.433)	
Mammography density	Fatty breast	11		0.642 (-1.418-2.124)	0.211
	Dense breast	89		1.255 (0.937-2.444)	
ER	Negative	40		1.05 (0.538-1.859)	0.074
	Positive	60		1.418	

			(0.967-2.451)	
PR	Negative	64	1.138 (0.741-2.298)	0.254
	Positive	36	1.462 (0.967-2.451)	
HER-2	Negative	63	1.288 (0.925-2.665)	0.175
	Positive	30	1.087 (0.776-1.752)	
	N/A	7		
Ki-67	Negative	36	1.555 (0.579-2.451)	0.384
	Positive	44	1.225 (0.928-1.779)	
	N/A	20		
Pathology	IDC	90	1.262 (0.816-2.467)	0.925
	ILC	2	1.188 (0.336-)	
	DCIS	8	1.189 (0.756-2.411)	
Nuclear grade	Not high	47	1.288 (0.769-2.384)	0.842
	High	46	1.225 (0.767-2.497)	
	N/A	7		
Histologic grade	Not high	57	1.288 (0.853-2.254)	0.722
	High	28	1.075 (0.676-4.031)	
	N/A	15		
Lymphovascular invasion	Absent	88	1.194 (0.741-2.319)	0.289
	Present	7	1.631 (1.292-2.580)	
	N/A	5		

*In one postmenopausal and another premenopausal woman, conductivity data of contralateral normal breast or tumor were lost due to processing error.

IV. Discussion

Composition of the epithelium and stromal breast tissue changed along with menstruation cycles due to hormonal change. In the proliferative phase, high estrogen levels induce interlobular stroma to become denser and more cellular. In the secretory phase, high progesterone levels induce interlobular stroma to become less cellular. Several studies have shown that hormonal variations according to menstrual cycles may be important factors causing increasing vascularization of the breast parenchyma and histamine-like effects such as vasodilation and increased vessel permeability [36-38]. Several studies have also reported change in water content within the breast according to menstruation cycle [39,40]. For these reasons, there is a possibility that the menopausal status and menstrual cycles influence BPE. So far, there have been different results among the studies looking at the effect of menstruation cycles on BPE [9,11-13]. A recent study that evaluated ADC and BPE of the normal breast parenchyma according to the menstruation cycle showed no difference in both ADC and BPE according to the menstruation cycle [41]. In our study, as recent studies [9,41], there was no significant difference in BPE according to menstruation cycles. These results suggest that the composition change of the breast tissue according to hormonal change is not enough to cause gross BPE changes. However, compared to the second week group with the lowest tendency of BPE and the fourth week group with the highest tendency, the fourth week group tends to have a lower percentage of BPE than the second week group. Both ADC and conductivity of the normal breast showed no significant difference, even when the ADC and conductivity were compared to the second and fourth week groups, respectively. Comparing the premenopausal and postmenopausal groups, BPE was significantly higher in the premenopausal group, and these results were consistent with those of previous studies [9,42]. Considering the above results, the change in breast composition according to

menopausal status is large enough to cause BPE changes, but the change according to menstruation cycles is not enough to cause BPE changes. In our study, there was no significant difference in ADCs of normal glandular tissue between premenopausal and postmenopausal women, which is inconsistent with results of previous studies showing that postmenopausal women had lower ADCs of normal glandular tissue than premenopausal women [19,43]. Recently, Shin et al. showed contralateral ADCs were significantly lower in fatty breast than those in dense breast and inferred that partial volume effect caused by the presence of fat might contribute to reduce the absolute ADCs in postmenopausal women compared with those in premenopausal women [44]. In our study, the proportion of fatty breast (23.9%) in postmenopausal women is lower than that in the study by Shin et al (37.3%). We surmise that the impact of the partial volume effect in our study was less than that in the previous study, which supports the hypothesis that ADCs of normal glandular tissue are more consistent in dense breast with less fat. In our study, there was no significant difference for ADCs of contralateral normal breasts according to menstrual cycles in premenopausal women, which is consistent with findings of previous studies [19,20,45]. A previous study in which eight healthy female subjects were scanned once a week for 4 weeks using DWI and evaluated normal variations in ADCs of breast parenchyma during menstrual cycle showed that the variation of ADC was only 5.5% across the menstruation cycle [45]. Based on our result and that of previous studies, although there are changes in the breast composition according to menstruation cycles, the change in ADCs of normal parenchyma according to menstruation cycles is considered insignificant. In our study, multivariate analysis showed that mammographic density had a positive correlation with ADC of normal glandular tissue, which was consistent with the findings of previous studies [46]. In our study, the ADC of contralateral normal breast had negative correlation to BMI, which is not reported in the previous literatures, to the best of our knowledge. However, one previous study reported

that ADCs were positively correlated to breast density [46] and another reported that breast density was negatively correlated with BMI [47]. Based on these results, we can infer that ADC can be negatively correlated to BMI, consistent with our results.

In our study, normalized ADCs of breast cancer did not significantly differ between premenopausal and postmenopausal women and among menstruation cycles in premenopausal women. These results were consistent with those of previous studies that showed no significant difference in normalized ADCs of breast cancer according to the menopausal status and menstruation cycles [19]. In multivariate analysis, normalized ADC was significantly higher in patients with marked parenchymal enhancement than in those with minimal parenchymal enhancement. A previous study showed that a higher degree of BPE was associated with a low ADCs of breast parenchyma [48]. Our study showed a similar tendency, but the results were not statistically significant. On the other hand, absolute ADCs of breast cancer showed a tendency to increase as parenchymal enhancement increased (B=48.544, p=0.129). Normalized ADC, the ratio of tumor ADC to parenchymal ADC, can be inferred to increase as the parenchymal enhancement increases, and the value was statistically significant in our study. Normalized ADC was significantly lower in patients with ER-positive cancer than in those with ER-negative cancer, which is consistent with the results of the previous study [49]. The ER-positive group often had high cellularity that could prevent the pathway of blood vessels and decrease blood perfusion, resulting in lower ADCs [50,51]. Mammographic density was an independent factor associated with normalized ADC. These results were inconsistent with those of previous studies showing positive correlation between ADC of contralateral normal breast and mammographic density, but normalized ADC did not show significant difference depending on mammography density [19]. Normalized ADCs (ADCs of breast cancer/ADCs of contralateral normal breast) are inversely proportional to ADC of contralateral

normal breast. In our study, ADCs of contralateral normal breast had positive correlation with dense breast on the mammogram, which is consistent with the findings of a previous study[19]. For this reason, dense breast on the mammogram had lower normalized ADCs. In univariate analysis, patients with PR-positive cancer showed lower normalized ADCs than those with PR-negative cancer. In our study, the proportion of patients with PR-positive cancer was higher in the premenopausal group than in the postmenopausal group. Premenopausal women had more dense breasts, and dense breasts had lower ADCs of contralateral normal breast. Normalized ADCs are inversely proportional to the ADCs of contralateral normal breast. Therefore, patients with PR-positive cancer had lower normalized ADCs. However, those factors were not independent after adjusting other factors, including mammographic density, in multivariate analysis.

When comparing conductivity of normal fibroglandular tissue between the premenopausal and postmenopausal groups using Mann-Whitney U test, there was no significant difference, although premenopausal women have higher conductivity values of contralateral normal breast. These results differed from the ADCs, which did not show any difference according to the menopausal status. In multivariate analysis, mammographic density was the only independent factor associated with conductivity of normal breast. Previous studies suggested that the average conductivity value of fat was less than that of breast parenchyma[25]. Therefore, dense breasts on the mammogram have higher conductivity than fatty breasts. We can refer to normalized conductivity that is unaffected by mammographic density. We surmise that the reason for higher conductivity in the premenopausal group than in the postmenopausal group is that the proportion of fatty breast in premenopausal group is lower than that in the postmenopausal group. Although ROIs are carefully drawn to avoid fatty tissue as much as possible, mammographic density may affect conductivity of contralateral fibroglandular tissue due to the partial volume effect. In our study,

menstruation cycles did not affect conductivity of normal breast. These results mean that in premenopausal women, it is possible to perform MRI analysis anytime regardless of the menstruation cycle. Our study is the first to evaluate the effect of menstruation cycles on conductivity of breast tissue. In univariate analysis, age was negatively correlated with conductivity of normal breast. However, age was not an independent factor associated with conductivity of contralateral fibroglandular tissue after adjusting for mammographic density through multiple linear regression analysis. Older women's breasts contain more fat than younger women's, and fat has a lower conductivity value than fibroglandular tissues. In line with this, BMI was negatively correlated with conductivity of normal breast. Breast density is negatively correlated with BMI, which is a reasonable result considering fat quantity. Considering mammographic density was the only independent factor affecting the conductivity of normal breast, the relationship between BMI and conductivity can be explained.

In our study, there was no significant difference in the normalized conductivity of breast cancer between premenopausal and postmenopausal women or according to the menstruation cycle. No factor was associated with normalized conductivity of breast cancer. Normalized conductivity values of breast cancer were significantly higher than those of contralateral fibroglandular tissue. These results suggest that diagnostic potential of normalized conductivity for the screening modality to identify the breast cancer without being affected by other clinicopathologic factors.

In our study, conductivity values of breast cancer were significantly higher than those of contralateral fibroglandular tissues. These results are consistent with those of a previous in-vivo study [25]. High conductivity of a malignancy is attributed to factors such as necrosis, increased sodium concentration, water, and cell membrane charge [30].

In our study, the proportion of patients with ER-positive and PR-positive cancer was higher in the premenopausal group than in the postmenopausal group. A previous study also showed the proportion of patients with PR-positive cancer was higher in the premenopausal group than in the postmenopausal group [19]. Several studies have suggested that younger women are more likely to have ER-negative breast cancer [52,53]. However, a study on Chinese women showed that patients aged <50 years had a higher proportion of ER-positive or PR-positive cancer, [54] which is consistent with our result. The result showing a higher proportion of dense breast and strong BPE in the premenopausal group than in the postmenopausal group was consistent with that in a previous study [42].

There were several limitations in our study. First, our study was retrospective and did not measure variations in the conductivity or ADCs in the same patient during menstruation cycles. However, our results agreed with those of previous prospective studies in which fluctuations in ADCs of breast parenchyma in the same patient were not significant during menstruation cycles [45]. Second, our study included a relatively small sample size. A larger sample size is needed to increase reliability of the results. Third, the image was only interpreted by two reviewers who formed a consensus prior to reporting the results. Fourth, we did not evaluate inter-observer agreement and intra-scan reproducibility. Further study should be need for clinical applications.

V. Conclusion

In conclusion, there was no significant difference in the contralateral and normalized ADCs and contralateral and normalized conductivity during the menstruation cycles, suggesting that MRI can be performed at any time regardless of the menstruation cycle. Conductivity of normal breast parenchyma is a factor that is not affected by other various clinocopathologic factors, except breast density.

Reference

1. Berg WA, Zhang Z, Lehrer D, Jong RA, Pisano ED, Barr RG, et al. Detection of breast cancer with addition of annual screening ultrasound or a single screening MRI to mammography in women with elevated breast cancer risk. Jama 2012;307:1394-404.
2. Saslow D, Boetes C, Burke W, Harms S, Leach MO, Lehman CD, et al. American Cancer Society guidelines for breast screening with MRI as an adjunct to mammography. CA: a cancer journal for clinicians 2007;57:75-89.
3. Kuhl CK, Schild HH. Dynamic image interpretation of MRI of the breast. Journal of Magnetic Resonance Imaging 2000;12:965-74.
4. Hunt CH, Hartman RP, Hesley GK. Frequency and severity of adverse effects of iodinated and gadolinium contrast materials: retrospective review of 456,930 doses. American Journal of Roentgenology 2009;193:1124-7.
5. Broome DR, Girguis MS, Baron PW, Cottrell AC, Kjellin I, Kirk GA. Gadodiamide-associated nephrogenic systemic fibrosis: why radiologists should be concerned. American Journal of Roentgenology 2007;188:586-92.
6. McDonald RJ, McDonald JS, Kallmes DF, Jentoft ME, Murray DL, Thielen KR, et al. Intracranial gadolinium deposition after contrast-enhanced MR imaging. Radiology 2015;275:772-82.
7. Radbruch A, Weberling LD, Kieslich PJ, Eidel O, Burth S, Kickingereder P, et al. Gadolinium retention in the dentate nucleus and globus pallidus is dependent on the class of contrast agent. Radiology 2015;275:783-91.
8. DeMartini WB, Liu F, Peacock S, Eby PR, Gutierrez RL, Lehman CD. Background parenchymal enhancement on breast MRI: impact on

diagnostic performance. American Journal of Roentgenology 2012;198:W373-W80.

9. Kang SS, Ko EY, Han BK, Shin JH, Hahn SY, Ko ES. Background parenchymal enhancement on breast MRI: influence of menstrual cycle and breast composition. Journal of Magnetic Resonance Imaging 2014;39:526-34.
10. Kamitani T, Yabuuchi H, Kanemaki Y, Tozaki M, Sonomura T, Mizukoshi W, et al. Effects of menstrual cycle on background parenchymal enhancement and detectability of breast cancer on dynamic contrast-enhanced breast MRI: A multicenter study of an Asian population. European journal of radiology 2019;110:130-5.
11. Müller-Schimpfle M, Ohmenhaüser K, Stoll P, Dietz K, Claussen CD. Menstrual cycle and age: influence on parenchymal contrast medium enhancement in MR imaging of the breast. Radiology 1997;203:145-9.
12. Delille JP, Slanetz PJ, Yeh ED, Kopans DB, Garrido L. Physiologic changes in breast magnetic resonance imaging during the menstrual cycle: perfusion imaging, signal enhancement, and influence of the T1 relaxation time of breast tissue. The breast journal 2005;11:236-41.
13. Kuhl CK, Bieling HB, Gieseke J, Kreft BP, Sommer T, Lutterbey G, et al. Healthy premenopausal breast parenchyma in dynamic contrast-enhanced MR imaging of the breast: normal contrast medium enhancement and cyclical-phase dependency. Radiology 1997;203:137-44.
14. Sardanelli F, Boetes C, Borisch B, Decker T, Federico M, Gilbert FJ, et al. Magnetic resonance imaging of the breast: recommendations from the EUSOMA working group. European journal of cancer 2010;46:1296-316.
15. Woodhams R, Matsunaga K, Shinichi K, Hirofumi H, OZAKI M, IWABUCHI K, et al. ADC mapping of benign and malignant breast

tumors. Magnetic resonance in medical sciences 2005;4:35-42.

16. Woodhams R, Matsunaga K, Iwabuchi K, Kan S, Hata H, Kuranami M, et al. Diffusion-weighted imaging of malignant breast tumors: the usefulness of apparent diffusion coefficient (ADC) value and ADC map for the detection of malignant breast tumors and evaluation of cancer extension. Journal of computer assisted tomography 2005;29:644-9.
17. Park MJ, Cha ES, Kang BJ, Ihn YK, Baik JH. The role of diffusion-weighted imaging and the apparent diffusion coefficient (ADC) values for breast tumors. Korean journal of radiology 2007;8:390-6.
18. Yabuuchi H, Matsuo Y, Sunami S, Kamitani T, Kawanami S, Setoguchi T, et al. Detection of non-palpable breast cancer in asymptomatic women by using unenhanced diffusion-weighted and T2-weighted MR imaging: comparison with mammography and dynamic contrast-enhanced MR imaging. European radiology 2011;21:11-7.
19. Shin S, Ko ES, Kim RB, Han B-K, Nam SJ, Shin JH, et al. Effect of menstrual cycle and menopausal status on apparent diffusion coefficient values and detectability of invasive ductal carcinoma on diffusion-weighted MRI. Breast cancer research and treatment 2015;149:751-9.
20. Kim JY, Suh HB, Kang HJ, Shin JK, Choo KS, Nam KJ, et al. Apparent diffusion coefficient of breast cancer and normal fibroglandular tissue in diffusion-weighted imaging: the effects of menstrual cycle and menopausal status. Breast cancer research and treatment 2016;157:31-40.
21. Surowiec AJ, Stuchly SS, Barr JR, Swarup A. Dielectric properties of breast carcinoma and the surrounding tissues. IEEE Transactions on Biomedical Engineering 1988;35:257-63.
22. Joines WT, Zhang Y, Li C, Jirtle RL. The measured electrical properties

of normal and malignant human tissues from 50 to 900 MHz. Medical physics 1994;21:547-50.

23. Haacke E, Petropoulos L, Nilges E, Wu D. Extraction of conductivity and permittivity using magnetic resonance imaging. Physics in medicine and biology 1991;36:723.
24. Katscher U, Djamshidi K, Voigt T, Ivancevic M, Abe H, Newstead G, et al. Estimation of breast tumor conductivity using parabolic phase fitting. Adapting MR in a Changing World: ISMRM 20th Annual Meeting, Melbourne, Australia, 5-11 May 2012: ISMRM (International Society Magnetic Resonance in Medicine); 2012.
25. Shin J, Kim MJ, Lee J, Nam Y, Kim Mo, Choi N, et al. Initial study on in vivo conductivity mapping of breast cancer using MRI. Journal of Magnetic Resonance Imaging 2015;42:371-8.
26. Voigt T, Katscher U, Doessel O. Quantitative conductivity and permittivity imaging of the human brain using electric properties tomography. Magnetic Resonance in Medicine 2011;66:456-66.
27. Katscher U, Kim D-H, Seo JK. Recent progress and future challenges in MR electric properties tomography. Computational and mathematical methods in medicine 2013;2013.
28. Kim SY, Shin J, Kim DH, Kim EK, Moon HJ, Yoon JH, et al. Correlation between electrical conductivity and apparent diffusion coefficient in breast cancer: effect of necrosis on magnetic resonance imaging. Eur Radiol 2018;28:3204-14.
29. Kim S-Y, Shin J, Kim D-H, Kim MJ, Kim E-K, Moon HJ, et al. Correlation between conductivity and prognostic factors in invasive breast cancer using magnetic resonance electric properties tomography (MREPT). European radiology 2016;26:2317-26.
30. Sha L, Ward ER, Stroy B. A review of dielectric properties of normal and malignant breast tissue. SoutheastCon, 2002. Proceedings IEEE:

IEEE; 2002. p.457-62.

31. Seo JK, Kim M-O, Lee J, Choi N, Woo EJ, Kim HJ, et al. Error analysis of nonconstant admittivity for MR-based electric property imaging. IEEE transactions on medical imaging 2012;31:430-7.
32. Lee J, Shin J, Kim DH. MR-based conductivity imaging using multiple receiver coils. Magnetic resonance in medicine 2016;76:530-9.
33. Morris E, Lee C. ACR BI-RADS® magnetic resonance imaging. ACR BI-RADS® atlas, Breast Imaging Reporting and Data System Reston. American College of Radiology 2013.
34. Yi M, Huo L, Koenig K, Mittendorf E, Meric-Bernstam F, Kuerer H, et al. Which threshold for ER positivity? A retrospective study based on 9639 patients. Annals of Oncology 2014;25:1004-11.
35. EI Khouli RH, Jacobs MA, Mezban SD, Huang P, Kamel IR, Macura KJ, et al. Diffusion-weighted imaging improves the diagnostic accuracy of conventional 3.0-T breast MR imaging. Radiology 2010;256:64-73.
36. Vogel PM, Georgiade N, Fetter B, Vogel F, McCarty Jr K. The correlation of histologic changes in the human breast with the menstrual cycle. The American journal of pathology 1981;104:23.
37. Potten CS, Watson R, Williams G, Tickle S, Roberts SA, Harris M, et al. The effect of age and menstrual cycle upon proliferative activity of the normal human breast. British journal of cancer 1988;58:163.
38. Longacre TA, Bartow SA. A correlative morphologic study of human breast and endometrium in the menstrual cycle. The American journal of surgical pathology 1986;10:382-93.
39. Graham S, Stanchev P, Lloyd-Smith J, Bronskill M, Plewes D. Changes in fibroglandular volume and water content of breast tissue during the menstrual cycle observed by MR imaging at 1.5 T. Journal of Magnetic Resonance Imaging 1995;5:695-701.
40. Fowler P, Casey C, Cameron G, Foster M, Knight C. Cyclic changes in

composition and volume of the breast during the menstrual cycle, measured by magnetic resonance imaging. BJOG: An International Journal of Obstetrics & Gynaecology 1990;97:595-602.

41. Jung Y, Jeong S, Kim JY, Kang DK, Kim TH. Correlations of female hormone levels with background parenchymal enhancement and apparent diffusion coefficient values in premenopausal breast cancer patients: effects on cancer visibility. European Journal of Radiology 2020:108818.
42. King V, Gu Y, Kaplan JB, Brooks JD, Pike MC, Morris EA. Impact of menopausal status on background parenchymal enhancement and fibroglandular tissue on breast MRI. European radiology 2012;22:2641-7.
43. O'Flynn EA, Morgan VA, Giles SL. Diffusion weighted imaging of the normal breast: reproducibility of apparent diffusion coefficient measurements and variation with menstrual cycle and menopausal status. European radiology 2012;22:1512-8.
44. Arens N, Bleyl U, Hildenbrand R. HER2/neu, p53, Ki67, and hormone receptors do not change during neoadjuvant chemotherapy in breast cancer. Virchows Archiv 2005;446:489-96.
45. Partridge SC, McKinnon GC, Henry RG, Hylton NM. Menstrual cycle variation of apparent diffusion coefficients measured in the normal breast using MRI. Journal of Magnetic Resonance Imaging: An Official Journal of the International Society for Magnetic Resonance in Medicine 2001;14:433-8.
46. Siraj Z, Klifa C, Carballido-Gamio J, Hylton N. Comparison of ADC values and MR breast densities in a normal population. Proc. Intl. Soc. Mag. Reson. Med; 1847. p.2005.
47. Gillman J, Chun J, Schwartz S, Schnabel F, Moy L. The relationship of obesity, mammographic breast density, and magnetic resonance

imaging in patients with breast cancer. Clinical imaging 2016;40:1167-72.

48. Kawamura A, Satake H, Ishigaki S, Ikeda M, Kimura R, Shimamoto K, et al. Prediction of background parenchymal enhancement on breast MRI using mammography, ultrasonography, and diffusion-weighted imaging. Nagoya journal of medical science 2015;77:425.

49. Meng L, Ma P. Apparent diffusion coefficient value measurements with diffusion magnetic resonance imaging correlated with the expression levels of estrogen and progesterone receptor in breast cancer: A meta-analysis. Journal of cancer research and therapeutics 2016;12:36.

50. Choi BB, Kim SH, Kang BJ, Lee JH, Song BJ, Jeong SH, et al. Diffusion-weighted imaging and FDG PET/CT: predicting the prognoses with apparent diffusion coefficient values and maximum standardized uptake values in patients with invasive ductal carcinoma. World journal of surgical oncology 2012;10:126.

51. Park SH, Choi HY, Hahn SY. Correlations between apparent diffusion coefficient values of invasive ductal carcinoma and pathologic factors on diffusion-weighted MRI at 3.0 Tesla. Journal of Magnetic Resonance Imaging 2015;41:175-82.

52. Tarone RE, Chu KC. The greater impact of menopause on ER–than ER+ breast cancer incidence: a possible explanation (United States). Cancer Causes & Control 2002;13:7-14.

53. Yerushalmi R, Gelmon KA, Leung S, Gao D, Cheang M, Pollak M, et al. Insulin-like growth factor receptor (IGF-1R) in breast cancer subtypes. Breast cancer research and treatment 2012;132:131-42.

54. Lian W, Fu F, Lin Y, Lu M, Chen B, Yang P, et al. The impact of young age for prognosis by subtype in women with early breast cancer. Scientific reports 2017;7:11625.

ABSTRACT(IN KOREAN)

자기공명전기물성단층촬영을 이용한 생체내 유방암 및 정상섬유유선 조직의 도전율 연구: 현성확산계수와의 비교

<지도교수 김민정>

연세대학교 대학원 의학과

원 소 연

월경 주기 또는 폐경 여부에 따른 정상섬유유선 조직의 도전율을 현성확산계수와 비교하여 평가하고 정상섬유유선 조직의 도전율이 유방암 환자에서 다른 임상병리적 인자들에 영향을 받는지를 밝히는 것이 목적이다.

이 연구는 월경에 대한 정보가 있고 2013년 7월과 2017년 12월 사이에 유방암의 수술전 평가를 위해 유방 자기공명영상을 촬영한 102명의 유방암 환자를 포함하였다. 종양의 정규화된 도전율및 현성확산계수와 반대쪽 정상섬유유선 조직의 도전율 및 현성확산계수가 측정되었으며 폐경 여부(폐경전과 폐경후 여성)와 월경주기(1주차-4주차)에 따라 비교하였다.

폐경전과 폐경후 여성사이에 반대측 정상섬유유선 조직

의 현성확산계수에는 유의한 차이가 없었으며(p=0.534) 폐경전 여성에서 월경 4주중 반대측 정상섬유유선 조직의 현성확산계수에는 유의한 차이가 없었다(p=0.534). 반대측 정상섬유유선 조직의 도전율은 폐경후 여성에서보다 폐경전 여성에서 더 높은 경향성을 보였으나 유의한 차이는 없었다 (p=0.057). 폐경전 여성에서 월경 4주중 정상 섬유유선조직의 도전율에는 유의한 차이가 없었다(p=0.800). 정규화된 도전율과 현성확산계수 둘 다 폐경전 여성과 폐경후 여성에서 유의한 차이는 없었으며 (p=0.920, p=0.259) 폐경전 여성에서 월경 4주간에도 유의한 차이는 없었다(p=0.147, p=0.949). 다변량 분석에서, 유방밀도는 반대측 정상 유방의 도전율과 연관된 독립적 인자였다 (p=0.001). 배경실질 조영, 에스트로겐 수용체와 유방밀도는 유방암의 정규화된 현성확산계수와 연관된 독립적인 인자였다 (p=0.001, p=0.013, p=0.034).

월경 주기동안 반대측 현성확산계수 및 유방암의 정규화된 현성확산계수와 반대측 도전율 및 유방암의 정규화된 도전율은 유의한 차이를 보이지 않았으며, 이는 자기공명영상을 월경 주기에 관계없이 어느 시기에나 촬영할 수 있다는 것을 시사한다. 정상 유방 실질의 도전율은 유방치밀도를 제외한 다른 여러 임상병리적 인자들에 영향을 받지 않았다.

핵심되는 말 : 자기공명전기물성단층촬영, 도전율, 현성확산계수, 정상 섬유유선 조직, 유방암, 월경주기, 폐경 여부